Improving energy efficiency of a bipedal walker with optimized nonlinear elastic coupling

Yinnan Luo[1], Ulrich J. Römer[1], Lena Zentner[2], and Alexander Fidlin[1]

[1] Institute of Engineering Mechanics, Karlsruhe Institute of Technology (KIT), Karlsruhe, Germany
[2] Compliant Systems Group, Ilmenau University of Technology, Ilmenau, Germany

Abstract. A method to improve the energy efficiency of a bipedal walking robot by means of nonlinear elastic couplings between the robot's thighs is presented. The robot model consists of five rigid segments which are connected by four actuated revolute joints in the hip and knees. The walking movement is generated and stabilized by a nonlinear controller based on the hybrid zero dynamics approach. The optimum walking gaits and the optimum characteristic of the elastic coupling are identified via numerical optimization whereby the energy consumption of locomotion is minimized. Different walking speeds from 0.2 m/s to 1.4 m/s are considered in the study. According to simulations, the optimal nonlinear elastic coupling reduces the mean energy consumption by 78 % over the range of investigated speeds. This is significantly better compared to the coupling with optimal linear torsion spring, which saves 62 % energy. The free oscillations frequency of the swing leg under influence of the elastic coupling is derived from a simplified pendulum model. This free oscillations frequency closely matches with the double step frequency of the robot at different walking speeds. The nonlinear elastic coupling gives the robot the capability to walk in resonance at different speeds with a very high energy efficiency.

Keywords: energy efficient robot, bipedal walking, numerical optimization

1 Introduction

Bipedal robots are capable of walking in many different environments and have therefore a wide range of applications. For example, humanoid robots are used for supporting rescue missions in many natural disaster scenarios that are demonstrated in the DARPA Robotics Challenge. Besides stabilizing the walking movements, improving the energy efficiency of locomotion is another major challenge in the development of these robots. An autonomous robot has to carry its energy source (e.g. a battery) which limits its operation time and range. Compared to humans, even the latest developed humanoid walking robots such as Boston Dynamics ATLAS and Honda Asimo show poorer energy efficiencies [1–3]. One of the main reasons of the less efficient walking lies on the control strategies,

whose major task is to generate and stabilize the walking motion. There are many strategies focusing on different goals: e.g. the zero moment point (ZMP) principle enforces a nearly static stability of each robot body during the movement [4–6]. The controller focuses on giving the robot the capability to interact with the environments but may sacrifice the energy efficiency of the periodic movements like walking or running [7–9].

Other control strategies make use of the robot's natural dynamics and allow for higher efficiencies. For example, hybrid zero dynamics (HZD) based controllers stabilize periodic walking movements of underactuated robots. The dynamics are similar to human walking which utilizes the system's natural dynamics to achieve a high efficiency. The system's natural dynamics, which are preserved due to the underactuation, are influenced by the mechanical design parameters. Coupling the robot's segments with linear elastic torsion springs significantly increases the energy efficiency [10–12]. A numerical optimization process simultaneously optimizes the walking gaits as well as the elasticity of the torsion spring to minimize the energy consumption of locomotion. This paper investigates the influence of the elastic coupling's nonlinearity on the efficiency of walking using cubic splines to describe and optimize the spring characteristics.

2 Model of the robot and the nonlinear spring

Since the energy efficiency of locomotion mainly depends on the motion in the walking direction [13, 14], the focus of the presented research lies on a planer robot model whose lateral stabilizations are not considered. The robot model consists of five rigid segments, representing an upper body, two thighs and two shanks, which are connected by ideal revolute joints. Four electric motors installed at each joint provide the driving torque for the motion. The robot's thighs are coupled by a nonlinear torsion spring, whose characteristics are described by cubic splines. The parameters of the cubic splines are considered as mechanical design parameters of the robot.

As depicted in Fig. 1, the robot has periodic walking gaits that can be mathematically described as a hybrid dynamic model including two alternating phases: a single support phase (SSP) and a double support phase (DSP). In both walking phases, point feet are modeled at the end of the shanks. Therefore, no torques can be transmitted between the contacting leg and the ground. In the SSP, the stance leg is in contact with the ground and the other leg swings forwards without scuffing. The contact of the stance foot is modeled as an ideal revolute joint without actuation, which gives the robot model one degree of underactuation. The continuous motion in the SSP is described via differential equations. In the DSP, a discrete mapping models an instantaneous impact of the swing leg with the ground; at the same time, the former stance leg lifts off. Physical conditions of walks without slipping, unilateral contacts and static frictions at the contacting feet are ensured through further constraints.

A nonlinear controller generates and stabilizes the periodic walking gaits, namely a limit cycle of the hybrid dynamic system [15, 16]. The angles of the

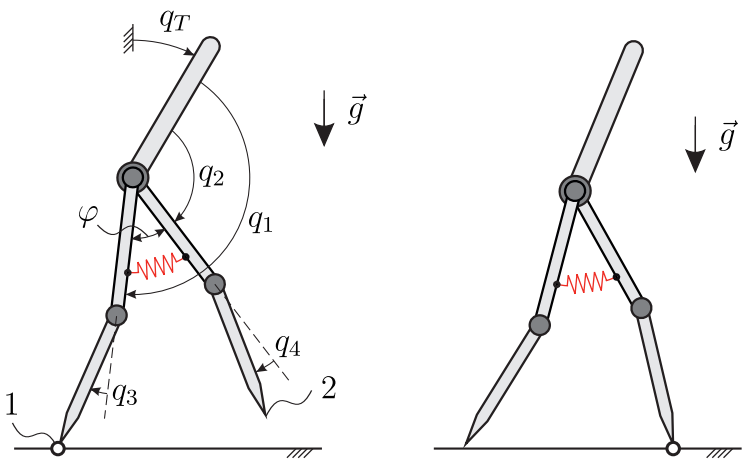

Fig. 1. Left: In the single support phase (SSP), leg 1 is in contact with the ground and leg 2 swings forwards. Right: In the double support phase (DSP), both legs instantaneously touch the ground. The former swing leg impacts the ground and the former stance leg lifts off.

Table 1. Model parameters

	upper body	thigh	shank	simplified model
moment of inertia (in kgm^2)	0.15	0.02	0.01	0.27
mass (in kg)	6.00	2.00	0.98	2.98
length (in m)	0.55	0.30	0.30	0.60
center of mass position (in m)	0.21	0.13	0.16	0.24

four actuated joints are synchronized to a set of time-invariant reference trajectories, described by Bézier polynomials with the parameters $\overline{\alpha}$. The remaining one degree of underactuation, namely the absolute rotation of the whole robot body about the contacting foot, is the controlled system's hybrid zero dynamics, if the error between the joint angles and the reference trajectories vanishes. Furthermore, the required driving torques $\overline{u} = [u_1, \ldots, u_4]^T$ in each electric motor are calculated through inverse dynamics, considering the elastic torques that are produced by the nonlinear torsion spring between the thighs.

In the mathematical description of the spring's nonlinearity, cubic splines show several advantages against high order polynomials. Cubic splines are smooth functions, combined by piecewise third-order polynomials, which pass through a set of control points (knots) [17]. Excluding the endpoints of the spline, whose second derivatives are set to zero, the first and the second derivatives of the knots are set equal to their neighborhoods. These boundary conditions uniquely define the complete spline, which is also known as a natural cubic spline.

It is assumed that the robot model is symmetric and its walking gaits are periodic. In this manner, the characteristic of the torsion spring between the thighs is supposed to be centrally symmetric. According to simulations, the maximal relative angle between the thighs of the robot without elastic couplings is 0.45 rad at the walking speed of 1.4 m/s. Thus, the active deflections of the nonlinear torsion spring are interpolated via splines in the interval of [-0.5, 0.5] rad; for larger deflections beyond this range a linear extrapolation is used. The spline is defined by a set of knots with the coordinates (φ_i, y_i) for $i = 0, ..., 10$: $[(-0.5, -m_5)$, $(-0.4, -m_4)$, $(-0.3, -m_3)$, $(-0.2, -m_2)$, $(-0.1, -m_1)$, $(0, 0)$, $(0.1, m_1)$, $(0.2, m_2)$, $(0.3, m_3)$, $(0.4, m_4)$, $(0.5, m_5)]$. The nonlinear characteristic $c(\varphi)$ of the nonlinear torsion spring has the property of central symmetry and is defined by the set of parameters $\overline{M}_{\mathrm{sp}} = (m_1, m_2, \ldots, m_5)^T$.

3 Simultaneous Optimization

Solving the closed loop walking motion is formulated as an optimization problem. On the one hand, the robot's walking gaits are defined by the Bézier parameters $\overline{\alpha}$; on the other hand, the nonlinear characteristics of the torsion spring are determined by the cubic spline with knots values $\overline{M}_{sp}$. While minimizing the energy consumption of walking, both parameter sets $\overline{\alpha}$ and $\overline{M}_{sp}$ are optimized simultaneously. The energy efficiency is optimized for different walking speeds form 0.2 m/s to 1.4 m/s. Sequential quadratic programming (SQP) is used as the optimization algorithms, which is mainly supported by the open source libraries "NLop.jl" and "OSQP.jl" in the programming language Julia. All derivatives required by the SQP algorithms are evaluated by automatic differentiation (AD) using the library "ForwardDiff.jl".

The objective of the numerical optimization is the energy consumption of locomotion. This is evaluated by a dimensionless quantity cost of transport (COT): the total supplied energy divided by the walking distance and the robot's weight. DC servo motors including gear transmissions convert the electrical energy into heat losses and mechanical energy. This work dosn't consider the heat losses, that are produced by the electric motor while it is maintaining static torques [11]. Furthermore, it is assumed that none of the generated electrical energy from the DC motors can be recovered during their braking operations (generator mode). So only positive mechanical power is considered in calculating

$$COT = \frac{\sum_{i=1}^{4} \int_0^{t^-} \max(u_i(t)\dot{q}_i(t), 0)\,\mathrm{d}t}{\ell_{\mathrm{step}} mg} \tag{1}$$

with the step length ℓ_{step} and the total weight of the robot mg.

The physical conditions, that are introduced in Section 2, are considered as constraints in the numerical optimization [10–12]. Besides the walking speed v, which is enforced by an equality constraint $g(x)$, other conditions are guaranteed through a set of inequality constraints $\overline{h}(x)$. These are unilateral ground contacts; the condition of static frictions at the contact; no scuffing of the swing foot and no hyperextension of the knees.

The characteristics of the torsion spring are assumed to be constant once it has been manufactured and assembled. On the other hand, the walking gaits can be changed by reprogramming the controller according to the desired operating states. To identify the optimal elastic coupling for a range of walking speeds, the mean COT by considering different walking speeds $\overline{V} = [v_1 = 0.2, v_2 = 0.3, \ldots, v_n = 1.4]$ m/s with the same spring characteristic is minimized. An optimization problem is formulated for each desired walking speed v_i with the constraits $g_i(x)$ and $\overline{h}_i(x)$. These problems are combined into an extended optimization problem with $x = [\overline{M}_{sp}, \overline{\alpha}_1, \ldots, \overline{\alpha}_n]$. In this way, a nonlinear torsion spring is identified that increases the overall energy efficiency at different walking speeds.

4 Results and discussion

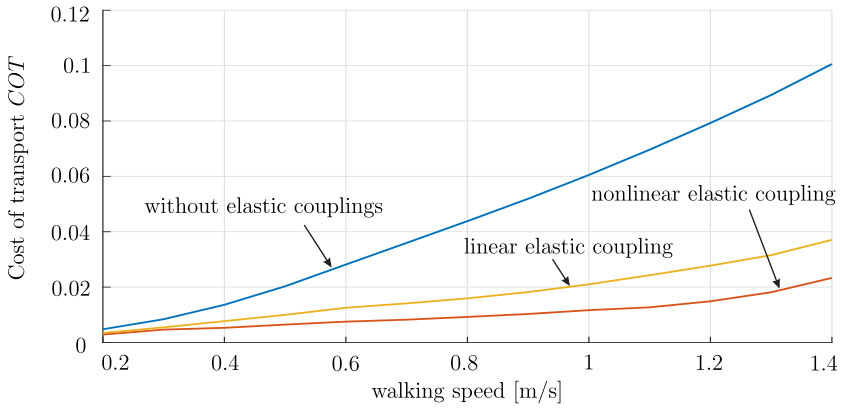

Fig. 2. The optimized cost of transport COT for different walking speeds from 0.2 m/s to 1.4 m/s with and without elastic couplings.

The nonlinear elastic coupling shows significant improvements even compared to a linear characteristic, as depicted in Fig. 2. In comparison to the robot without any elastic couplings, the mean energy consumption is reduced by 78 % for the investigated walking speeds. This is significantly better than using linear torsion springs, which results in a mean reduction of 62 %. In Fig. 2, COT represents the total positive mechanical work that is supplied to the walking system from electric motors for compensating the energy losses to maintain the periodic walking gaits. From the aspect of the energy balance, less energy losses results in a high energy efficiency using nonlinear springs. Besides, the maximal power of the electric motors is also reduced through the elastic coupling: without torsion springs the total maximal electrical power of four DC motors is 157.70

W at the speed 1.4 m/s; this is reduced to 71.63 W by using nonlinear springs. This makes the downsizing of the electric motors possible in an early development stage of any bipedal robots.

The optimal characteristic of the nonlinear torsion spring $c(\varphi)$ (the optimal parameter set $\overline{M}_{sp} = [-1.89, -6.89, -24.82, -183.35, -798.69]^T$ Nm) and the optimal stiffness ($k = 120.44$ Nm/rad) of the linear torsion spring are presented in Fig. 3. The deflections of the elastic couplings are equivalent to the relative angle φ between the thighs, which can be derived from the kinematical relationships. The simulations generally show an approximately linear relationship between the maximum relative angle of the thighs to the walking speed. At the walking speed of 1.4 m/s, the maximal deflection angle of the nonlinear torsion spring is 0.36 rad, which becomes 0.10 rad at 0.2 m/s; in the case of the optimal linear torsion spring, 0.33 rad is reached at 1.4 m/s and 0.05 at 0.2 m/s.

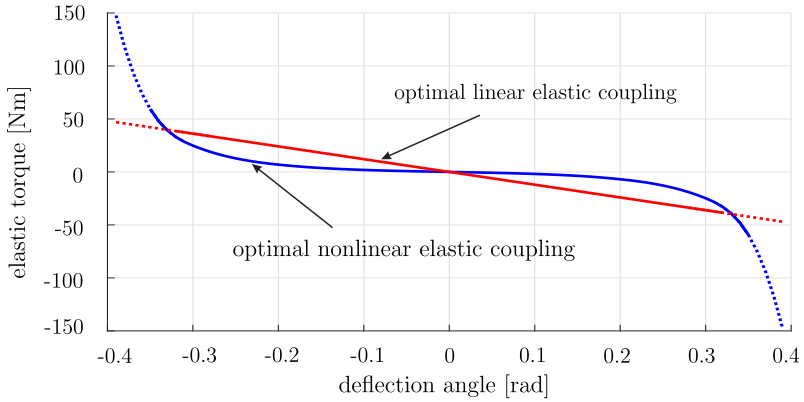

Fig. 3. The optimized linear and nonlinear torsion springs. The active operating ranges of the springs are plotted with solid lines.

During one step, the optimal nonlinear torsion spring provides little elastic torques at smaller deflection angles, where the swing leg finds itself in the swing period. At the beginning as well as the end of the step, the deflection angle reaches its maximum in this step and the elastic torque increases dramatically. This implies that the nonlinear spring tends to be activated only at the beginning and the end of the step. According to the studies about the normal human walk in [18] and [19], the muscles of the swing leg are mainly activated just right at the beginning and end of one step. During the swing period in the middle of this step, the muscles are normally inactive. In this sense, the optimized nonlinear torsion spring acts in a way similar to the human muscles. The natural dynamics of the swing leg are less suppressed through a nonlinear torsion spring during the swing period. Also, this leads to a larger step length and therefore less steps required

for the same walking distance: 0.20 m for using nonlinear torsion springs at the speed of 1.4 m/s; 0.18 m for linear torsion springs. The increased elastic torque decelerates the movement right before the swing leg touches the ground. In this process, kinetic energy is stored as potential energy into the torsion spring, which is reused for accelerating the robot at the beginning of the next step.

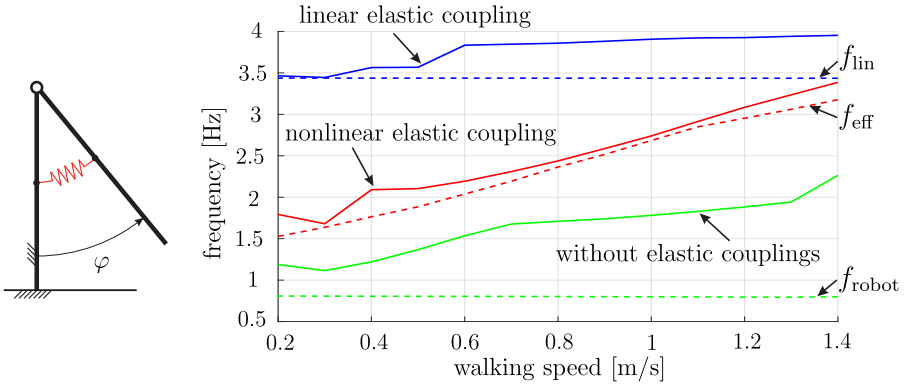

Fig. 4. Left: Simplified pendulum model for the analysis of the free oscillations frequency of the system consisting of two rigid bodies coupled by a nonlinear torsion spring. Right: Comparison of the derived free oscillations frequency of the pendulum model (dashed line) to the double step frequency of the complete robot (solid line).

A closer study on the walking motion is employed based on a simplified compound pendulum model in Fig. 4: both stance and swing leg are considered as rigid rods, whose mechanical parameters are derived from the thigh and shank of the formal complete robot model in Table 1. The stance leg is assumed to be firmly attached to the ground and connected to the swing leg by the torsion spring that is introduced in Fig. 3. The characteristic of the torsion spring therefore determines the free oscillations frequency of the simplified pendulum model. As the cubic spline $c(\varphi)$ is defined by piecewise cubic polynomials, the potential energy of the nonlinear spring is evaluated via integration:

$$V(\varphi) = -\int_0^{\varphi} c(\varphi)\,\mathrm{d}\varphi. \tag{2}$$

No energy dissipation is considered, the sum of the kinetic energy and the potential energy is constant

$$\frac{1}{2}J_o\dot{\varphi}^2 + mgr(1-\cos(\varphi)) + V(\varphi) = mgr(1-\cos(\varphi_{\text{MAX}})) + V(\varphi_{\text{MAX}}) \tag{3}$$

with the maximal deflection φ_{MAX} of the spring, where the velocity $\dot{\varphi}(\varphi_{\text{MAX}}) = 0$ and $J_o = J_{smp} + m_{smp}r_{smp}^2$, with the model parameters given in Table 1. The

angular velocity $\dot{\varphi}$ is then given by

$$\dot{\varphi} = \sqrt{\frac{2(mgr(\cos(\varphi) - \cos(\varphi_{\mathrm{MAX}})) + V(\varphi_{\mathrm{MAX}}) - V(\varphi))}{J_o}}. \tag{4}$$

The swing period $\frac{T}{4}$, starting from the position $\varphi(0) = 0$ and ending at $\varphi(\frac{T}{4}) = \varphi_{\mathrm{MAX}}$, of this nonlinear system can be determined via numerical integration

$$\frac{T}{4} = \int_0^{\varphi_{\mathrm{MAX}}} \frac{1}{\dot{\varphi}} \,\mathrm{d}\varphi = \sqrt{\frac{J_o}{2}} \int_0^{\varphi_{\mathrm{MAX}}} \frac{1}{\sqrt{mgr(\cos(\varphi) - \cos(\varphi_{\mathrm{MAX}})) + V(\varphi_{\mathrm{MAX}}) - V(\varphi)}} \,\mathrm{d}\varphi. \tag{5}$$

The effective free oscillations frequency is given by $f_{\mathrm{eff}} = \frac{1}{T}$. The effective frequencies for the linear torsion spring f_{lin} and without any elastic coupling f_{robot} also follow from equation (5) by changing the elastic potential energy $V(\varphi)$ accordingly.

As depicted in Fig. 4, the double step frequencies of the optimized gaits using nonlinear springs are very close to the effective frequency f_{eff} of the corresponding pendulum model at different walking speeds, i.e. at different amplitudes of the spring. In contrast, the pendulum model containing linear or no springs has an almost constant free oscillations frequency due to small oscillations amplitude. Studies in [20] and [21] approach a nearly linear relationship between the step frequency and the walking speed according to observations of the normal human walk. Thus, the major effect of the optimized nonlinear torsion spring is that the walking gaits and the characteristics of the spring are simultaneously optimized in such a way, that the robot always walks near the resonance of the system even at different walking speeds with a very high efficiency.

Fig. 5 illustrates that both linear and nonlinear torsion springs reduce the energy losses while walking. These consist of two parts: the energy losses caused by the inelastic impact of the swing leg on the ground in the DSP, and the generated electrical energy from the electric motors in their braking operations, which is mainly turned into heat. Since the periodic walking gaits are limit cycles of the controlled system, any energy which is removed from the system due to braking or impact losses has to be supplied by the electric motors at some time. In all considered cases in Fig. 5, the impact losses are minimized by the optimization algorithm. After the numerical optimization, the robot always brakes its motion right before the impact in order to minimize the impact losses. This braking torque must be provided through the electric motors in the case that the robot has no elastic couplings. As described in Fig. 3, the spring contributes to the braking operations at the right moments which greatly reduces the required energy input by the electric motors.

5 Conclusion

A method to improve the energy efficiency of a bipedal walking robot is investigated using nonlinear torsion springs characterized by cubic splines to couple its thighs. The underactuated robot is controlled by a nonlinear controller based on

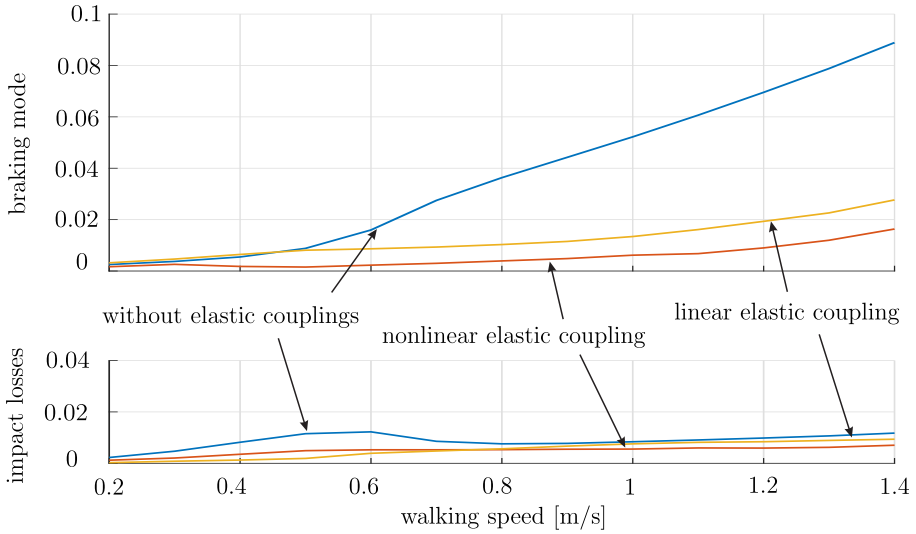

Fig. 5. Top: Removed energy due to the braking mode of the electric motors. Bottom: Energy losses due to the impact of the swing leg on the ground.

the hybrid zero dynamics approach. Its periodic walking gaits and the nonlinearity of the spring are determined simultaneously via numerical optimization, during the process of minimizing the energy consumption. Through the optimized nonlinear torsion spring, the mean energy consumption for walking speeds from 0.2 m/s to 1.4 m/s is reduced by 78 %. This is significantly better than an optimal linear spring that reduces 62 % of energy for the same conditions. The nonlinear spring tends to be activated only at the beginning and the end of one step, and remains silent during the swing period of the swing leg, which functions in a way similar to the human muscles. The free oscillations frequency of the swing leg is derived from a simplified pendulum model that is connected to the environment over the nonlinear spring. The free oscillations frequency of the pendulum model closely matches with the double step frequencies of the robot, that has optimum gaits generated by the optimization, i.e. the robot walks in resonance to achieve a very high energy efficiency at different walking speeds. According to simulations, not only the optimal step lengths but also step frequencies increase at larger walking speeds. This is in accordance with the studies about the relationship between the normal human step frequency and walking speeds.

In future works, the nonlinear elastic couplings between the other segments of the robot will be investigated. The nonlinear characteristics are supposed to be realized in praxis through compliant smart mechanisms [22]. The simulation results will be validated on a prototype of the robot with the real nonlinear torsion springs.

Acknowledgements: This work is financially supported by the German Research Foundation (DFG), grant FI 1761/4-1 | ZE 714/16-1.

References

1. S. Cotton, I.M. C. Olaru, M. Bellman, T.V.D. Ven, J. Godowski, and J. Pratt, 2012 IEEE International Conference on Robotics and Automation (2012).
2. A. Mazumdar, S. J. Spencer, C. Hobart, J. Salton, M. Quigley, T. Wu, S. Bertrand, J. Pratt, and S. P. Buerger, IEEE/ASME Transactions on Mechatronics 22(2), 898–908 (2017).
3. N. Kashiri, A. Abate, S. J. Abram, A. Albu-Schaffer, P. J. Clary, M. Daley, S. Faraji, R. Furnemont, M. Garabini, H. Geyer, and et al., Frontiers in Robotics and AI 5 (2018).
4. K. Hirai, M. Hirose, Y. Haikawa, and T. Takenaka, Proceedings. 1998 IEEE International Conference on Robotics and Automation (1998).
5. K. Nishiwaki, S. Kagami, Y. Kuniyoshi, M. Inaba, and H. Inoue, IEEE/RSJ International Conference on Intelligent Robots and System (2002).
6. M. Vukobratovic and B. Borovac, I. J. Humanoid Robotics 1(03), 157–173 (2004).
7. A.D. Kuo, IEEE Robotics Automation Magazine 14(2), 18–29 (2007).
8. S. Collins, A. Ruina, R. Tedrake, and M. Wisse, Science 307(5712), 1082–1085 (2005).
9. H. Shin and B.K. Kim, IEEE Transactions on Industrial Electronics 62(4), 2277–2286 (2015).
10. F. Bauer, U. J. Römer, A. Fidlin, and W. Seemann, Nonlinear Dynamics 83(3), 1275–1301 (2015).
11. F. Bauer, U. J. Römer, A. Fidlin, and W. Seemann, Multibody System Dynamics 38(3), 227–262 (2016).
12. U. J. Römer, C. Kuhs, M. J. Krause, and A. Fidlin, 2016 IEEE International Conference on Robotics and Automation (ICRA) (2016).
13. L. Tesio, D. Lanzi, and C. Detrembleur, Clinical Biomechanics 13(2), 77–82 (1998).
14. L. Tesio and V. Rota, Frontiers in Neurology 10 (2019).
15. E. Westervelt, J. Grizzle, and D. Koditschek, IEEE Transactions on Automatic Control 48(1), 42–56 (2003).
16. C. Chevallereau, G. Abba, Y. Aoustin, F. Plestan, E.R. Westervelt, C. Canudas-De-Wit, and J.W. Grizzle, IEEE Control Systems Magazine 23(5), 57–79 (2003).
17. E. W. Weisstein, MathWorld–A Wolfram Web Resource. URL https://mathworld.wolfram.com/CubicSpline.html (2020).
18. D. Winter and H. Yack, Electroencephalography and Clinical Neurophysiology 67(5), 402–411 (1987).
19. S. Mochon and T.A. Mcmahon, Journal of Biomechanics 13(1), 49–57 (1980).
20. D.W. Grieve and R. J. Gear, Ergonomics 9(5), 379–399 (1966).
21. J. E.A. Bertram, Journal of Experimental Biology 208(6), 979–991 (2005).
22. M. Zirkel, Y. Luo, U. J. Römer, A. Fidlin, and L. Zentner, Mechanisms and Machine Science, (2020) (accepted for publication).